AD-A107 715 DREXEL UNIV PHILADELPHIA PA DEPT OF PHYSICS AND ATMOS--ETC F/G 20/6
AN INVESTIGATION OF VARIABLE COHERENCE SOURCES & OF SOME PRACTI--ETC(U)
NOV 81 L M NARDUCCI, J D FARINA DAAG29-80-K-0001

UNCLASSIFIED ARO-17514.1-P NL

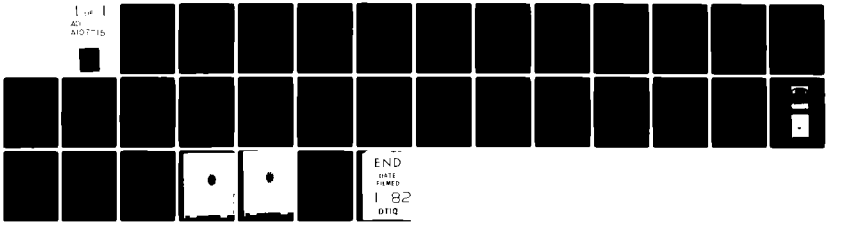

UNCLASSIFIED
SECURITY CLASSIFICATION OF THIS PAGE (When Data Entered)

ARO 17514.1-P

REPORT DOCUMENTATION PAGE	READ INSTRUCTIONS BEFORE COMPLETING FORM
1. REPORT NUMBER	2. GOVT ACCESSION NO. AD-A107715 (12) / 3. RECIPIENT'S CATALOG NUMBER
4. TITLE (and Subtitle) DAAG29-80-K-0001 An Investigation of Variable Coherence Sources & of Some Practical Applications	5. TYPE OF REPORT & PERIOD COVERED Final Report
	6. PERFORMING ORG. REPORT NUMBER
7. AUTHOR(s) Lorenzo M. Narducci, and James D. Farina	8. CONTRACT OR GRANT NUMBER(s) DAAG29-80-K-0001
9. PERFORMING ORGANIZATION NAME AND ADDRESS Physics & Atmospheric Science Department, Drexel University, Philadelphia, PA 19104	10. PROGRAM ELEMENT, PROJECT, TASK AREA & WORK UNIT NUMBERS
11. CONTROLLING OFFICE NAME AND ADDRESS U. S. Army Research Office Post Office Box 12211 Research Triangle Park, NC 27709	12. REPORT DATE
	13. NUMBER OF PAGES
14. MONITORING AGENCY NAME & ADDRESS (if different from Controlling Office)	15. SECURITY CLASS. (of this report) Unclassified
	15a. DECLASSIFICATION/DOWNGRADING SCHEDULE

16. DISTRIBUTION STATEMENT (of this Report)

Approved for public release; distribution unlimited.

NOV 25 1981

17. DISTRIBUTION STATEMENT (of the abstract entered in Block 20, if different from Report)

NA

18. SUPPLEMENTARY NOTES

The view, opinions, and/or findings contained in this report are those of the author(s) and should not be construed as an official Department of the Army position, policy, or decision, unless so designated by other documentation.

19. KEY WORDS (Continue on reverse side if necessary and identify by block number)

Coherence, Interferometry, Quasi-Homogeneous Sources

20. ABSTRACT (Continue on reverse side if necessary and identify by block number)

See Next Page

DD FORM 1 JAN 73 1473 EDITION OF 1 NOV 65 IS OBSOLETE

UNCLASSIFIED
SECURITY CLASSIFICATION OF THIS PAGE (When Data Entered)

20. ABSTRACT

We have investigated, designed and tested a modified form of Mach-Zehnder interferometer for measuring the coherence length of a partially coherent source. The instrument is unique in that it allows the recording of a fringe pattern and the extraction of the corresponding visibility curve even for sources with poor spatial coherence by virtue of the instrument's differential magnification. To our knowledge, the idea of magnifying a coherence pattern is new and could have important laboratory applications.

Final Report

AN INVESTIGATION OF VARIABLE COHERENCE SOURCES AND OF SOME PRACTICAL APPLICATIONS

Lorenzo M. Narducci

James D. Farina

November 9, 1981

U.S. Army Research Office

DAAG29-80-K-0001

Department of Physics & Atmospheric Science
Drexel University

A

1. Introduction

It is now well established both theoretically and experimentally[1-10] that the requirement of beam-like propagation for an optical field does not carry the full spatial coherence of the source as a necessary condition. Rather, it is entirely possible for a two-dimensional planar source to be globally incoherent, and yet to generate radiant fields whose far field intensity distrubition is confined within a relatively narrow solid angle.

This beam-like quality, in particular, is characteristic of a certain class of globally incoherent sources known under the name of quasi-homogeneous, or Collett-Wolf sources. Among their interesting properties, a remarkable reciprocity theorem has attracted considerable attention in view of its possible practical applications. This theorem insures the existence of a Fourier transform relation between the far field coherence function and the source intensity profile, on the one hand, and the far field angular intensity distribution and the near field coherence, on the other[1-5]. Thus, remarkably, the far field pattern, for example, carries no information on the near field intensity distribution.

The non-intuitive nature of this result was investigated rather extensively in our laboratory and confirmed to an excellent approximation[10]. Additional properties of the near, far and intermediate radiation field[11], were all found to be in excellent agreement with the assumed quasi-homogeneous nature of our source (an especially prepared glass surface illuminated by a He-Ne laser beam). Of course, a direct test of

quasi-homogeneity requires the experimental verification of the above mentioned reciprocity relation; because our early tests[10] were only concerned with the proof of the independence of the far field angular intensity profile, and not on the direct measurement of the source coherence function and its Fourier transform, much of the follow-up work has focused with the more difficult problem of the measurement of spatial coherence.

Because of the fine grained structure of our quasi-homogeneous source, it became rapidly clear in the early stages of this work that conventional methods for measuring spatial coherence, (e.g., by a fringe visibility with a reversing front Michelson interferometer) would suffer greatly from resolution limitations. The typical coherence length for our laboratory sources was inferred from far field pattern measurements, to be only of the order of several tens of microns.

One of the present principal investigators (JDF) conceived of the idea of designing an optical system that was capable of magnifying the visibility pattern, while maintaining its shape unchanged.

To this purpose, a conventional Mach-Zehnder interferometer was modified as discussed in Section 2 by inserting a pair of lenses along each of the two paths of the instruments, in such a way as to maintain an imaging relation between the entrance and exit planes of the device for both sets of imaging systems.

As shown in Section 2 and confirmed experimentally (in Section 3) if the ratio of the magnifications of the two imaging systems is made sufficiently close to unity, the entire set of fringes in the exit plane of the interferometer can be stretched spatially, and, thus, the resolution process can be aided considerably.

The modified Mach-Zehnder interferometer can now be claimed to be an effective laboratory tool for the study of fields with limited coherence length. The possibility of adapting this diagnostic technique outside the controlled laboratory environment does not look very promising; however, the study of sources with variable coherence or with specific coherence properties can now be undertaken with reasonable ease and accuracy even if the conditions are not at all amenable to a direct and conventional recording of the visibility function.

In Section 4 of this report, we describe the results of a study in which speckle reduction was obtained by illumination of a target with a beam of relatively high intensity but with global spatial incoherence.

2. Analytical Description of the Modified Mach-Zehnder Interferometer

An ordinary Mach-Zehnder interferometer has the structure shown in Figure 1. Two partially transmitting (1,3) and two highly reflecting (2,4) surfaces separate and recombine an incident wavefront. A difference between the paths can be introduced by a slight tilt of one of the beam splitters, although a controlled variation is somewhat time consuming to obtain and to maintain because of the spatial separation of the paths.

Usually a Mach-Zehnder interferometer is especially useful to observe density variations in gas-flow patterns. One beam passes through the optically flat windows of the test chamber, while the other beam traverses appropriate compensator plates. The resulting distortion of the wavefront will generate the desired fringe contour[12].

Under these conditions, the coherence properties of a wave field at the entrance plane of the interferometer do not differ significantly from those at the exit plane, save for possible degradation suffered by the beam inside the system, or because of the small propagation effects along the two paths. (The spatial coherence properties of an extended source improve as the wavefield propagates farther away from the source.)

For our purposes, it is very significant to note how the presence of a suitably chosen pair of optical elements (e.g., thin lenses), properly placed along the two optical paths can produce a significant "magnification" of the fringe visibility pattern at the exit plane of the instrument.

To show how this effect comes about, it is convenient to analyze the two-path interferometer as if the field propagation took place along

two separate straight segments as shown in Figure 2. Each path contains two thin lens elements of focal lengths f_1, f_2 and f_1', f_2, respectively. Each pair of lenses is positioned so that the entrance and exit planes of the interferometer satisfy the imaging condition for the selected values of the focal lengths and relative positions of the elements.

The field propagation through each path can be easily described in terms of the usual Fourier optics methods[13]. The analysis becomes especially transparent if one first maps each two-lens system into an equivalent thick lens characterized by principal planes H_1, H_2 and H_1', H_2', respectively, and effective focal lengths f and f', with[12]

$$\frac{1}{f} = \frac{1}{f_1} + \frac{1}{f_2} - \frac{\overline{H_1 H_2}}{f_1 f_2}$$

and

$$\frac{1}{f'} = \frac{1}{f_1'} + \frac{1}{f_2} - \frac{\overline{H_1 H_2}}{f_1' f_2}$$

Given a field amplitude distribution $E_0(x,y)$ at the entrance plane of the interferometer, the exit fields at the output plane have the form[13]

$$E(x_4, y_4) = \left(-\frac{ik}{2\pi}\right)^2 \frac{e^{ikL}}{(\ell_2 + H_1)(\ell_3 - H_2)} \int dx_3\, dy_3\, dx_1\, dy_1 \times$$

$$\exp\left\{\frac{ik}{2(\ell_3 - H_2)}\left[(x_4 - x_3)^2 + (y_4 - y_3)^2\right]\right\} \exp\left[-\frac{ik}{2L}(x_3^2 + y_3^2)\right] \times$$

$$\exp\left\{\frac{ik}{2(\ell_1 + H_1)}\left[(x_3 - x_1)^2 + y_3 - y_1)^2\right]\right\} E_0(x_1, y_1)$$

$$E(x_4,y_4) = -\frac{k^2}{4\pi^2} \frac{e^{[illegible]}}{(z_1-H_1')(z_3-H_2')} \iiiint dx_1\, dy_1\, dx_3\, dy_3$$

$$\exp\left\{\frac{ik}{2(z_3-H_2)}\left[(x_4-x_3)^2+(y_4-y_3)^2\right]\right\} \exp\left[-\frac{ik}{2f}(x_3^2+y_3^2)\right]$$

$$\exp\left\{\frac{ik}{2(z_1-H_1)}\left[(x_3'-x_1)^2+(y_3'-y_1)^2\right]\right\} E_0(x_1,y_1)$$

where the meaning of the various distances and the positions of the principal planes are illustrated in Figure 2, and where all the distances are measured relative to the appropriate principal planes. The fields $E(x_4,y_4)$ and $E'(x_4,y_4)$ differ from one another, of course, because of the different imaging properties of the two paths of the interferometer.

The total field at the exit plane (x_4,y_4) is given by

$$E_T = E + E'$$

and the total intensity is

$$I_T = \langle |E|^2 \rangle + \langle |E'|^2 \rangle + 2\,\mathrm{Re}\,\langle E E'^* \rangle$$

The coherence properties of the output field are described by the correlation function $\langle E E'^* \rangle$. This is given explicitly by the following multidimensional integral

$$\langle E E^{*} \rangle = \left(\frac{k}{2\pi}\right)^{2} \frac{}{(\ell_3 - H_2)^2 (\ell_1 + H_1)^2 (\ell_2 - H_2)^2 (\ell_3 - H_2')^2} \int dx_1\, dx_2\, dx_3\, dx_3'$$

$$\int dy_1\, dy_2\, dy_3\, dy_3' \exp\left\{ \frac{ik}{2(\ell_3 - H_2)} (x_1 - x_2)^2 - \frac{ik}{2f} x_3^2 + \frac{ik}{2(\ell_1 + H_1)} (x_3 - x_1)^2 \right\} \times$$

$$\exp\left\{ -\frac{ik}{2(\ell_3 - H_2')} (x_2 - x_3')^2 + \frac{ik}{2f'} x_3'^2 - \frac{ik}{2(\ell_1 + H_1)} (x_3' - x_1')^2 \right\} \times$$

$$\exp\left\{ \frac{ik}{2(\ell_3 - H_2)} (y_1 - y_2)^2 - \frac{ik}{2f} y_3^2 + \frac{ik}{2(\ell_1 + H_1)} (y_3 - y_1)^2 \right\} \times$$

$$\exp\left\{ -\frac{ik}{2(\ell_3 - H_2')} (y_2 - y_3')^2 + \frac{ik}{2f'} y_3'^2 - \frac{ik}{2(\ell_1 + H_1)} (y_3' - y_1')^2 \right\} \times$$

$$\langle E_0(x_1, y_1) E_0^{*}(x_1', y_1') \rangle ,$$

where the only variables that are affected by the ensemble average are the input field amplitudes. Under most conditions of interest, the input field correlation function can be expected to be spatially isotropic. Thus, the multidimensional integral splits up into the product of two similar integrals over the x and y integration variables, respectively. The first factor can be cast into the form:

$$\Gamma_x = \int \cdots dx_3\, dx_2\, dx_1\, dx_1'$$

$$\exp\left\{ \frac{i k}{2(\ell_2 - H_2)} x_2^2 + \frac{i k}{2} x_3^2 \left(\frac{1}{\ell_3 - H_2} - \frac{1}{f} + \frac{1}{\ell_1 + H_1} \right) \right.$$

$$\left. + \cdots \right\} = \cdots$$

$$\exp\left\{ \cdots \right\} \cdots$$

where $g_x(x_1 - x_1')$ denotes the field correlation function at the input plane for the spatial separation $(x_1 - x_1')$.

Because of the imaging conditions

$$\frac{1}{\ell_3 - H_2} - \frac{1}{f} + \frac{1}{\ell_1 + H_1} = 0$$

$$\frac{1}{\ell_3 - H_2'} - \frac{1}{f'} + \frac{1}{\ell_1' + H_1'} = 0$$

the integral simplifies considerably. For all practical purposes, the range of integration can be assumed to be infinite under the conditions of interest; thus, the x part of the integral takes the form

$$I_x = (2\pi)^2 \int dx_1\, dx_1' \sum_{-} k\left(\frac{x_4}{\ell_3 - H_2} + \frac{x_1}{\ell_1 + H_1}\right) \cdot$$

$$\delta\left[k\left(\frac{x_4}{\ell_3 - H_2'} + \frac{x_1}{\ell_1 + H_1'}\right)\right] \exp\left\{\frac{ik}{2(\ell_3 - H_2)} x_4^2 - \frac{ik}{2(\ell_3 - H_2')} x_4^2\right\} \cdot$$

$$\exp\left\{\frac{ik}{2(\ell_1 - H_1)} x_1^2 - \frac{ik}{2(\ell_1 + H_1')} x_1'^2\right\} \cdot \Im_x (x_1 - x_1')$$

The result can now be cast in closed form for an arbitrary input correlation function.

$$I_x = \frac{2\pi}{k})^2 (\ell_1 + H_2)(\ell_1' + H_1') \cdot \Im_x\left[\left(\frac{\ell_1 + H_1}{\ell_3 - H_2} - \frac{\ell_1' + H_1'}{\ell_3 - H_2'}\right) x_4\right] \cdot$$

$$\exp\left\{\frac{ik}{2} x_4^2 \left(\frac{1}{\ell_3 - H_2} - \frac{1}{\ell_3 - H_2'} + \frac{\ell_1 + H_1}{(\ell_3 - H_2)^2} - \frac{\ell_1' + H_1'}{(\ell_3 - H_2')^2}\right)\right.$$

As a result, the required total correlation function takes the form

$$\langle E E^* \rangle = \frac{(\ell_1 + H_2)(\ell_1 + H_1')}{(\ell_3 - H_2)(\ell_3 - H_2')} \Im_x\left[\left(\frac{\ell_1 + H_2}{\ell_3 - H_2} - \frac{\ell_1' + H_1'}{\ell_3 - H_2'}\right) x_4\right] \cdot$$

$$\Im_y\left[\left(\frac{\ell_1 + H_1}{\ell_3 - H_2} - \frac{\ell_1 + H_1'}{\ell_3 - H_2'}\right) y_4\right] \cdot$$

$$\exp\left[\frac{ik}{2} x_4^2 + y_4^2\right)\left(\frac{1}{\ell_3 - H_2} - \frac{1}{\ell_3 - H_2'} + \frac{\ell_1 + H_2}{(\ell_3 - H_2)^2} - \frac{\ell_1' + H_1'}{(\ell_3 - H_2')^2}\right.$$

At this point, we recognize that the transverse magnification of the two lens pairs are given by

$$M^{-1} = -\frac{d_2 - f_2}{f_2 - d_2}$$

$$M'^{-1} = -\frac{d_2 + H_2}{f_2 - H_2'}$$

Hence, the propagation through the interferometer has the effect of changing the linear scale of the input correlation function by a factor M_{eff} given by

$$\left| \frac{1}{M_{eff}} \right| = \left| \frac{1}{M} - \frac{1}{M'} \right|$$

This implies that if M is chosen to be close to M' the effective magnification of the output correlation function M_{eff} can be made quite large. In particular, if the input correlation has polar symmetry (as most correlation functions of experimental interest are expected to have), the output field correlation will also display a polar symmetry, i.e.,

$$\Gamma(x_1, y_1) = \Gamma\left[\left|\frac{1}{M} - \frac{1}{M'}\right| (x_2^2 + y_2^2)^{1/2}\right]$$

The role of the "stretching" factor M_{eff} is to magnify the fringe structure at the output of the device so that higher resolution can be obtained. In effect, the interferometer takes a given input visibility curve and maps it into the output plane with a magnification M_{eff} of all details.

It follows at once that if σ_c is the correlation length of the input field, the output correlation length is given by

$$\sigma_c^{out} = \sigma_c \Big/ \left| \frac{1}{M} - \frac{1}{M'} \right|$$

Note also that if one choses, as in our experimental set up, $\ell_1 = f_1$, $\ell_3 = f_2$, $\ell_1' = f_1'$ we have the useful relations

$$\frac{\ell_2 + H_1}{\ell_3 - H_2} - \frac{\ell_1' + H_1'}{\ell_3 - H_2'} = \frac{f_1 - f_1'}{f_2}$$

$$\frac{1}{\ell_3 - H_2} - \frac{1}{\ell_3 - H_2'} + \frac{\ell_1 + H_1}{(\ell_3 - H_2)^2} - \frac{\ell_1 + H_1}{(\ell_3 - H_2')^2} = \frac{f_1}{f_2 f'^2} - \frac{f_1'}{f_2 f'^2}$$

3. Design and Operation of the Modified Mach-Zehnder Interferometer

a) Alignment and Calibration Procedure

In order to obtain meaningful data for sources possessing coherence widths of the order of a few tens of microns, the resolution requirements of the imaging system of the interferometer must be made rather stringent. In our case, the required resolution was obtained by using lenses which were nearly diffraction limited achromatic doublets similar to those commonly found as objectives in good quality refracting telescopes. The lenses were 2" in diameter and with focal lengths of 10" and 11", respectively, yielding f-numbers of about 5. This choice proved adequate, if not ideal for all our measurements.

In order to maintain an f#5 system, it became necessary to insure that the limiting apertures of the interferometer were the lens apertures themselves. For this reason, the mirrors and beamsplitters were designed to have 4-5" diameters. Because of the large diameter of these elements, their thickness was chosen proportionally large so as to provide structural stability on an interferometric scale.

In fact, the original version of the interferometer was built with beam splitters and mirrors 0.75 inches thick. The preliminary tests of the instrument revealed significant aberrations in the imaging due to the large thickness of the glass plates. In a subsequent version of our design, this problem was corrected by replacing the entrance beamsplitter with a 6 μm pellicle. This produced excellent imaging but at the expense of a new problem. The acoustic noise which is practically unavoidable in our laboratory was seen to produce a complete obscuration of the fringes because of the pellicle vibrations. Only after great care was applied

to isolate the pellicle acoustically, the fringes were made stationary for times of the order of several seconds. This was ample time to obtain a record of the fringe pattern by normal photographic techniques.

The alignment and calibration of the modified Mach-Zehnder interferometer represented a considerable effort. The best procedure was found to consist of the following steps.

1) A preliminary alignment is to be carried out as with an ordinary Mach-Zehnder interferometer.

2) The lenses are placed in their appropriate positions within the device and their fine setting adjusted in such a way that a point source (microscope objective) in the object plane produces a collimated beam after the light traverses each lens. The difficulty with this procedure is that it must be carried out simultaneously in both legs without moving the point source. At this point, the distance between the point source and each of the lenses is equal to the respective focal lengths. Thus, in all subsequent discussion, the object plane is defined as the plane containing the point source and oriented perpendicular to both axes of symmetry of the lenses.

3) At this point, it is necessary to place the final imaging lens just after the last beam splitter of the interferometer. The position of this lens relative to the first two inside the interferometer is arbitrary because its role is to image two objects (the images of the first lenses) at infinity.

4) With the point source in the object plane, it is now necessary to identify the final image plane. This is done by observing the image of the point source through a microscope. This shows two images with

only one in focus at a given time as a result of collimation errors in Step 2. It is now necessary to choose one of the images and to hold the microscope to a sharp focus with respect to the selected image. The lens corresponding to the unfocused image is adjusted longitudinally until focusing is achieved for both images.

Once this step is accomplished, the object and final image planes are defined for the remainder of the measurement. This completes the alignment procedure.

Our experience shows that this measurement requires great care and that it should be repeated several times (about five times) in order to insure reliability.

b) Measurements of microscopic spatial coherence functions.

Once the modified Mach-Zehnder interferometer has been properly aligned and calibrated, the measurement of the spatial coherence function of a source is relatively easy to perform. The partially coherent source is placed in the previously defined object plane and the visibility of the fringes in the image plane is observed.

It is important to note that as long as the observation of fringes is conducted in the image plane of the instrument, then the visibility of the fringes is governed solely by the coherence of the source in the object plane. This implies that if the partially coherent source is placed out of the object plane, e.g., further removed from the interferometer, then the visibility of the fringes in the image plane is a measure of the coherence of the field which has propagated from the source to the object plane.

By taking advantage of this observation we were able to measure the evolution of the coherence function at increasing distance from the source.

The sources used in our measurements were the quasi-homogeneous sources described in Ref. 10. Excellent correlation was found between the coherence lengths estimated in Ref. 10 using the reciprocity theorems mentioned in Section 1, and those measured directly with the modified Mach-Zehnder interferometer.

Typical fringe patterns obtained with the source at various distances from the object plane are shown in Figure 3. We define $\sigma(z)$ as the full width of the degree of spatial coherence at a distance z from the source. The behavior of $\sigma(z)$ is shown in Figure 4 for a range of distances up to 20 cm. The extrapolated value of $\sigma(z)$ for $z \to 0$ was defined to be 13 μm. This compares very favorably with the value of about 10 μm obtained from the far field intensity measurements described in Ref. 10.

4. Speckle Pattern Reduction

A well known manifestation of the spatial coherence of an optical beam is the granular appearance of an illuminated spot on a rough surface. The effect is a very easy one to display, and can provide a nice pedagogical demonstration. However, it is also a considerable nuisance when dealing with coherently illuminated systems. The cure is rather simple: all one needs to do is to switch from a laser to a normal incoherent source for the illumination. However, this also has the effect of lowering the brightness of the illuminated spot unless special attention is taken to collimating the source field.

The globally incoherent nature of a quasi-homogeneous source, coupled to its highly directional emission property, provides a useful combination to reduce or to eliminate the speckle effect while maintaining adequate illumination of the target. Because of the size of the grain speckles grows as the width of the spatial coherence function, then by varying the spatial coherence properties of the light, the speckle size can be increased or reduced accordingly.

In order to demonstrate this effect, we have first illuminated a page of text using light directly from a c.w. laser and recorded the speckle photographically. Then we have placed a rotating phase screen (quasi-homogeneous source) between the laser and the target and recorded the new speckle pattern. In the first case, the large width of the spatial coherence function produced a speckle pattern that was large enough to make the illuminated text almost unreadable.

In the second case instead, and using the same camera aperture (f32) the text material became quite readable (Fig. 5a,b).

It should be kept in mind that because the degree of spatial coherence is responsible for the effect, the procedure described in this section of the report would not produce a significant improvement on the speckle pattern for a target placed in the far field of the source. However, certain applications which do not require large distances between source and illuminated areas will benefit from the use of quasi-homogeneous sources instead of the commonly used laser beams.

FIGURE 1

Schematic representation of a Mach-Zehnder interferometer. 0 represents an extended source in the object plane; 1 and 3 represent partially transmitting and 2.4 totally reflecting surfaces; I denotes the image plane and L_1,L_1' and L_2 are the three lenses that are used in our modified form of the interferometer.

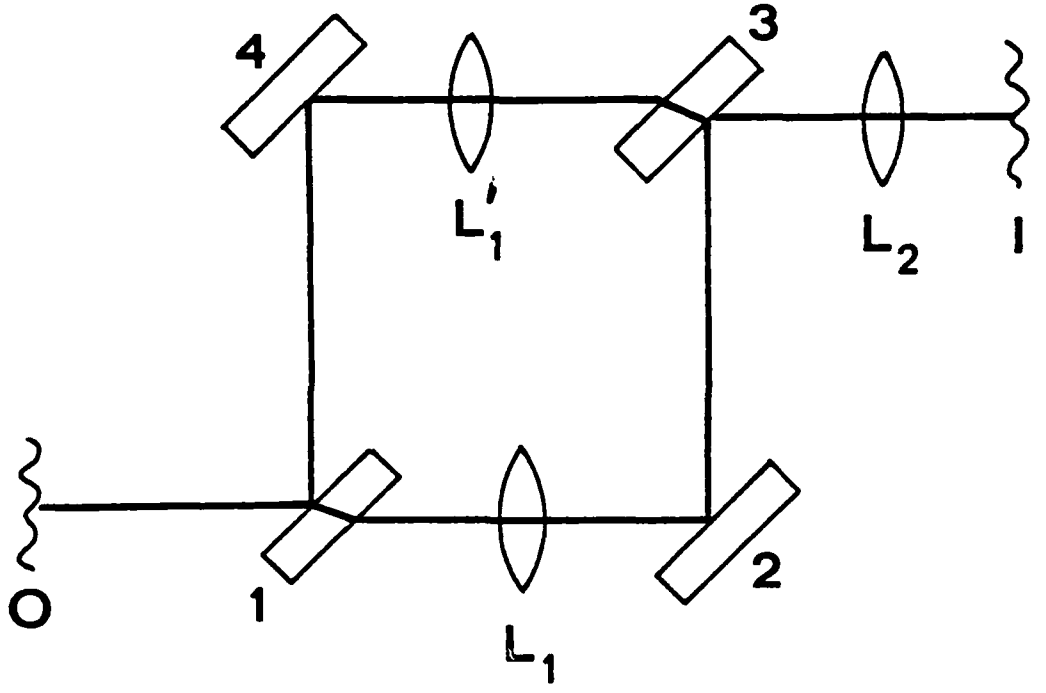

FIG.1

FIGURE 2

Schematic representation of the interferometer; the top and bottom part of the figure display the two optical paths separately. The distances are labelled by the same symbols used in the mathematical description of Section 2 of this report.

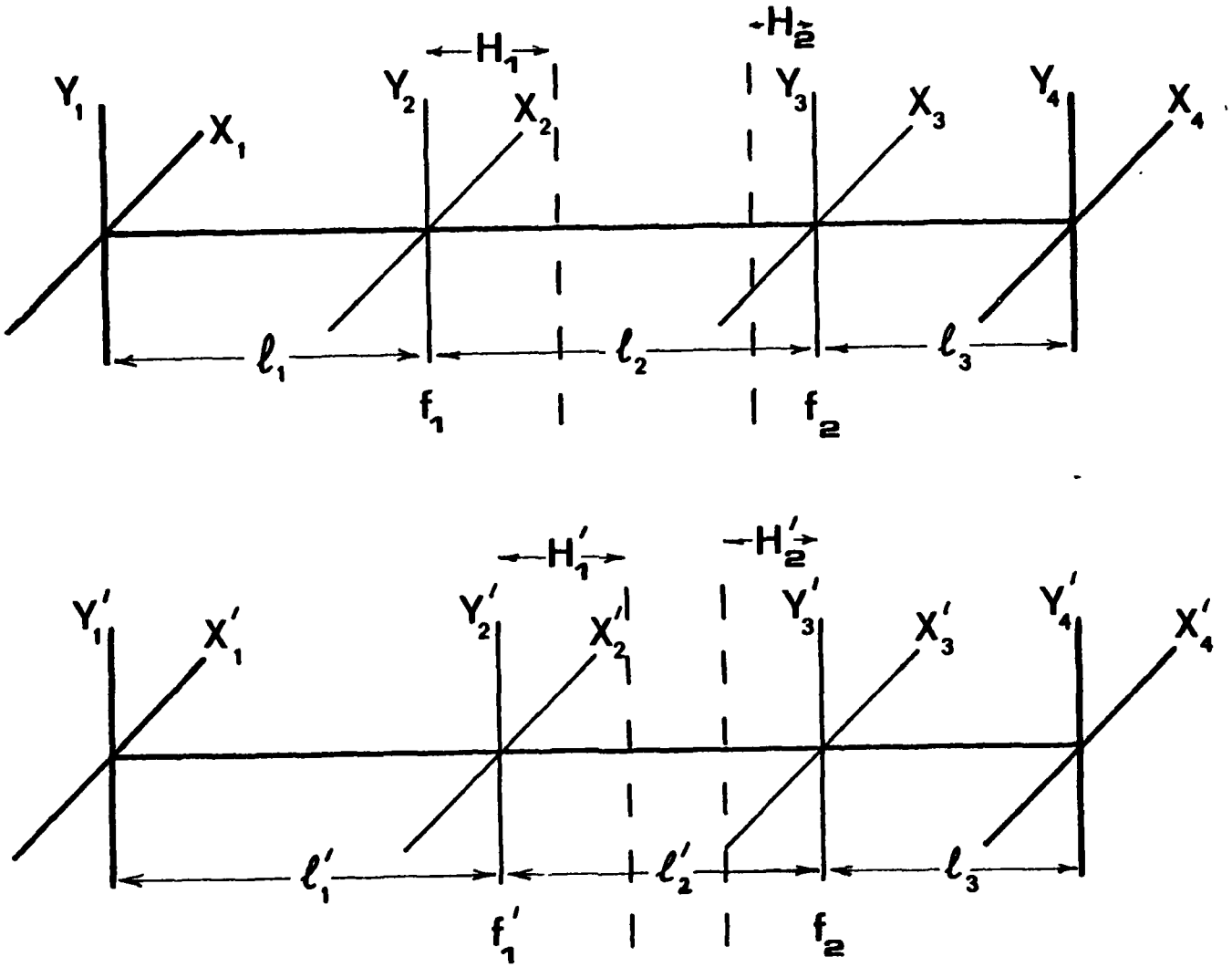
H1
H2
Y1
X1
Y2
X2
Y3
X3
Y4
X4
ℓ1
ℓ2
ℓ3
f1
f2
H'1
H'2
Y'1
X'1
Y'2
X'2
Y'3
X'3
Y'4
X'4
ℓ'1
ℓ'2
ℓ3
f'1
f2

FIG. 2

FIGURE 3

Two examples of fringe patterns observed through the microscope. The top figure corresponds to a distance between the source and the object plane of 9 cm, the bottom to 20 cm. There is a very noticeable increase in the vertical range of the visibility curve.

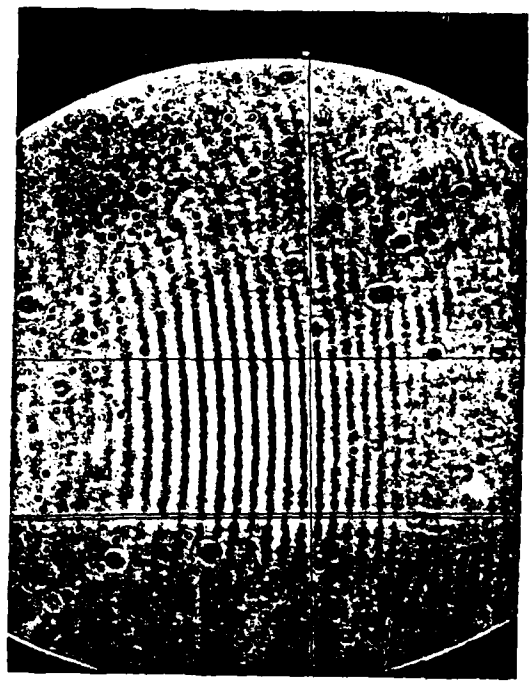

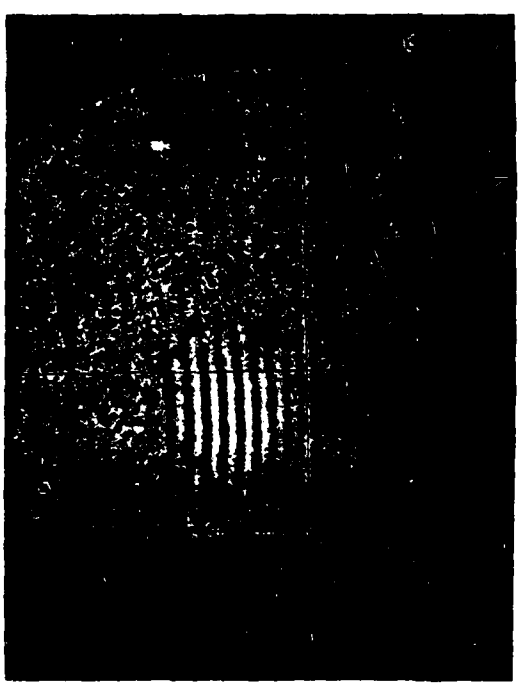

FIGURE 4

Behavior of the coherence length as a function of distance from the source plane. The vertical axis is measured in arbitrary units. After calibration, the coherence length corresponding to z = 0 has been found to by 13 μm. The horizontal axis is measured in cm.

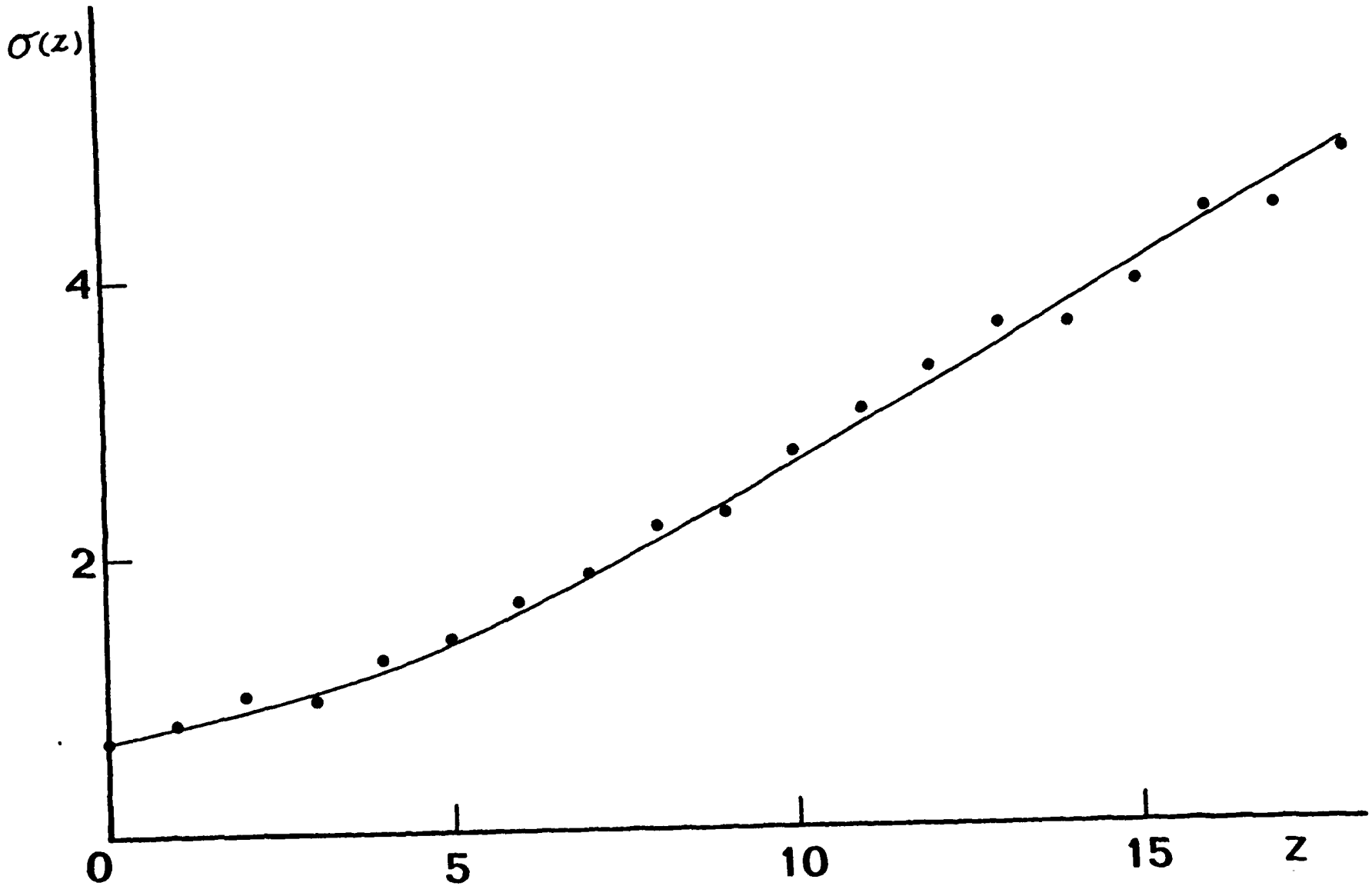

FIG. 4

FIGURE 5

Speckle pattern reduction (a) target is illuminated with a He-Ne laser beam; (b) target is illuminated with the beam from a quasi-homogeneous source.

entury mon
his F [illegible]
amplitude of

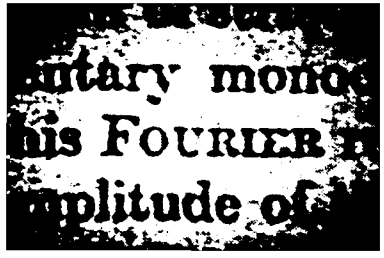
ntary mono
is FOURIER
plitude of

REFERENCES

1. E. Collett and E. Wolf, Opt. Lett. 2, 27 (1978).
2. E. Wolf, and E. Collett, Optics Comm. 25, 293 (1978).
3. E. Collett and E. Wolf, J. Opt. Soc. Am. 69, 942 (1979).
4. W.H. Carter and E. Wolf, J. Opt. Soc. Am., 67, 785 (1977).
5. W.H. Carter and E. Wolf, Opt. Comm., 25, 288 (1978).
6. H.P. Baltes and B. Steinle, Nuovo Cimento 41, 428 (1977).
7. F. Gori, C. Palma, Opt. Comm. 27, 185 (1978).
8. P. De Santis, F. Gori, C. Palma, Opt. Comm. 28, 151 (1979).
9. P. De Santis, F. Gori, G. Guattari, C. Palma, Opt. Comm. 29, 256 (1979).
10. J.D. Farina, L.M. Narducci, E. Collett, Opt. Comm. 32, 203 (1980).
11. J.T. Foley and M.S. Zubairy, Opt. Comm. 26, 297 (1978).
12. E. Hecht and A. Zajac, Optics, Addison-Wesley Publishing Company, 1976.
13. J.W. Goodman, Introduction to Fourier Optics, McGraw-Hill, NY, 1968.


DA
FILM